Draft: Isotopic-constrained atmospheric carbon budget

Deliverable 1.3

Authors: Sebastian Lienert, Thomas Frölicher, Fortunat Joos

Document Information

GRANT AGREEMENT	821003
PROJECT TITLE	Climate Carbon Interactions in the Current Century
PROJECT ACRONYM	4C
PROJECT START DATE	1/6/2019
RELATED WORK PACKAGE	WP1
RELATED TASK(S)	T1.1.2
LEAD ORGANIZATION	UBERN
AUTHORS	Sebastian Lienert, Thomas Frölicher, Fortunat Joos
SUBMISSION DATE	23.11.2020
DISSEMINATION LEVEL	PU / CO / DE

History

DATE	SUBMITTED BY	REVIEWED BY	VISION (NOTES)
27/11/2020	S. Lienert (UBERN)	P. Friedlingstein (UNEXE)	

Please cite this report as: Lienert, S., Frölicher, T. L., Joos, F., (2020), Draft: Isotopic-constrained atmospheric carbon budget, D1.3 of the 4C project

Disclaimer: The content of this deliverable reflects only the author's view. The European Commission is not responsible for any use that may be made of the information it contains.

Table of Contents

List of figures

About 4C

Climate-Carbon Interactions in the Coming Century (4C) is an EU-funded H2020 project that addresses the crucial knowledge gap in the climate sensitivity to carbon dioxide emissions, by reducing the uncertainty in our quantitative understanding of carbon-climate interactions and feedbacks. This will be achieved through innovative integration of models and observations, providing new constraints on modelled carbon-climate interactions and climate projections, and supporting Intergovernmental Panel on Climate Change (IPCC) assessments and policy objectives.

Executive Summary

One of the key goals of WP1 is the establishment of novel observational constraints to further improve our quantitative understanding of the global carbon cycle. Here, we present our progress towards realizing a constraint using $^{13}CO_2$. We are using the LPX-Bern DGVM to simulate the land carbon cycle and Bern3D for the ocean carbon cycle. We discuss multiple changes to the model structure of LPX-Bern that were needed to accurately simulate $^{13}CO_2$. We report progress on the simulation of the seasonal cycle of $\delta^{13}C(CO_2)$, as well as the simulation of the overall atmospheric $^{13}CO_2$ budget. UBern is on track to realize the goals set in task T1.1.3.

Keywords

Carbon-cycle, observational constraints, 13C, carbon isotopes.

1 Model Development

In order to use atmospheric measurements of $^{13}CO_2$ as an observational constraint for carbon-cycle simulations, the capabilities of the used models to simulate isotope processes must be assessed and improved. We use the isotope-enabled Earth system Model of Intermediate Complexity (EMIC) Bern3D-LPX (Ritz *et al.*, 2011; Menviel, Joos and Ritz, 2012). In the following, we focus on the land component of the EMIC, the Dynamic Global Vegetation Model (DGVM) LPX-Bern v1.4 (Lienert and Joos, 2018). While the model performs well in an evaluation with tree-ring-based carbon isotope measurements (Keller *et al.*, 2017), we discovered that further changes in the model code are needed to enable the comparison with atmospheric $^{13}CO_2$ data. In the following subsections, we describe the implemented changes in LPX-Bern.

1.1 Distribution of C3 and C4 plants

The isotopic signature of the land-biosphere is of vital importance to the seasonal cycle and overall inventory of atmospheric $\delta^{13}C(CO_2)$. The plant isotopic signature strongly depends on vegetation composition. It is especially important to accurately capture the relative abundance of herbaceous C_3 and C_4 plants since the difference in their respective photosynthetic pathways leads to a significant difference in isotopic fractionation. C_3 plants are overall more abundant, but the drought and high-temperature resistance of C_4 plants have led to them being used extensively in agriculture (e.g. maize or sugarcane). The LPX-Bern model overestimates the fraction of C_4 plants, leading to a too positive plant isotopic signature. This shortcoming has been overcome by explicitly considering C_3 and C_4 crop types and a slight model parameter adjustment.

In the unmodified version of LPX-Bern v1.4, the model determines the area fraction of C_3 and C_4 plants dynamically based on bioclimatic limits and competition for resources. These processes are regulated with Plant Functional Types (PFTs) specific parameters. For the cropland land-use class, empiric information on the distribution of crops is available (Hurtt *et al.*, 2020). By introducing an additional crop land-use class and having both crop land-use classes contain only C_3 or C_4 crops, it is possible to explicitly prescribe the maximum C_3 and C_4 area fractions from the LUH2 forcing dataset (Hurtt *et al.*, 2020). However, if environmental conditions are unfavorable, the model will not utilize all the available area, resulting in a mismatch. This was the case for some regions in the subtropics, where the parameterization of C_3 plants did not allow for growth, highlighting the need for change in parameterization. Multiple factorial simulations revealed that the maximum transpiration rate E_{max}, regulating the water supply to a plant (Sitch *et al.*, 2003), was a suitable parameter for adjustment. By increasing E_{max} from 5 mm day^{-1} to 7 mm day^{-1} for C_3 plants the agreement with observations was further enhanced.
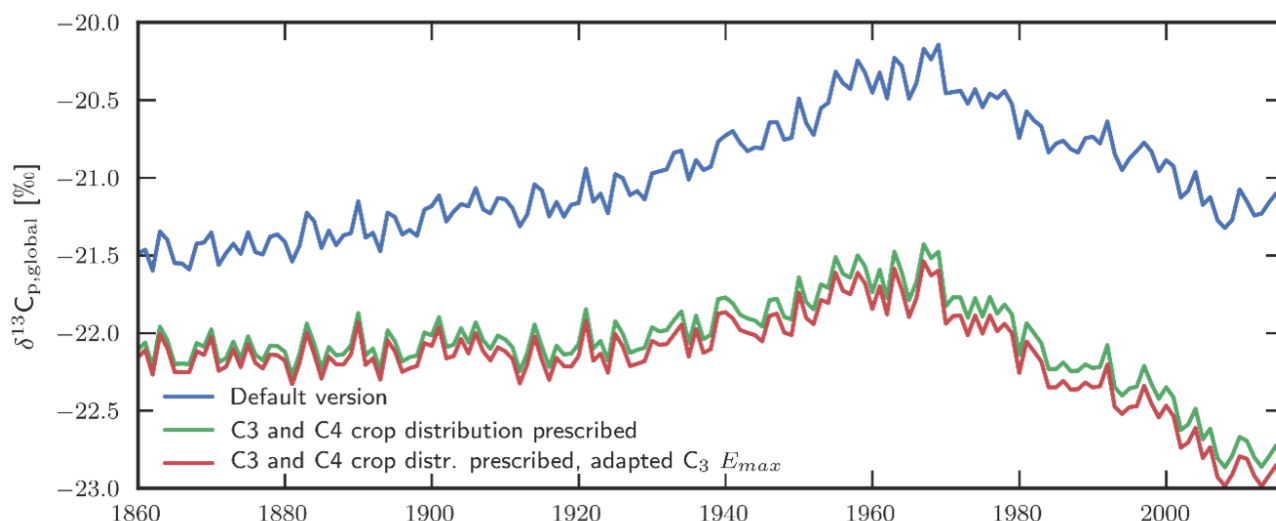
Figure 1: The globally integrated annual isotopic signature at leaf level $\delta^{13}C_{p,global}$ over the historical period. In blue the unmodified version of LPX-Bern v1.4 is shown. In green, a simulation using a modified version of LPX-Bern v1.4, including two separate land-use classes for C₃ and C₄ crops is displayed. The red line corresponds to a simulation with an additional adjustment to the PFT parameter E_{max}.

The effect of the C₃ and C₄ crop distribution on the global carbon assimilation signature $\delta^{13}C_{p,global}$ is shown in Figure 1. The model version with prescribed C₃ and C₄ crop area fraction produces on average a 1.1‰ lower signature than the unmodified version. The adaptation of the E_{max} parameter introduces a further decrease in the signature.

The global assimilation weighted discrimination averaged from 1860 to 2016 is 14.3‰ for the unmodified version, 15.4‰ for the version distinguishing C₃ and C₄ land-use classes, and 15.5‰ for the version with adapted C₃ E_{max} parameter. The values of the modified versions are closer to the literature range of 15.7‰ to 18.1‰ (Suits *et al.*, 2005; Scholze, Ciais and Heimann, 2008), albeit still slightly smaller. For now, only the C₄ plants in agriculture are considered. However, C₄ plants also grow on natural soils. Going forward, the parametrization of herbaceous PFTs on mineral soils may have to be adjusted as well.

1.2 Ensuring internal model consistency

In LPX-Bern's development history, carbon isotopes were added fairly early (Scholze *et al.*, 2003). Internally, information about the ^{13}C content of pools and fluxes is stored using the δ-notation, i.e. only the ratio of ^{13}C to ^{12}C relative to a standard is stored. While this notation is very convenient when dealing with discrimination processes (e.g. during photosynthesis), it is prone to introduce very small book-keeping errors. These are not important when analyzing $\delta^{13}C$ in the land biosphere. However, when assessing the small trends in atmospheric $\delta^{13}CO_2$ arising from changes on land, the land biosphere ^{13}C accounting must be accurate and relative deviations between integrated fluxes and inventory changes should be less than order 10^{-5}.
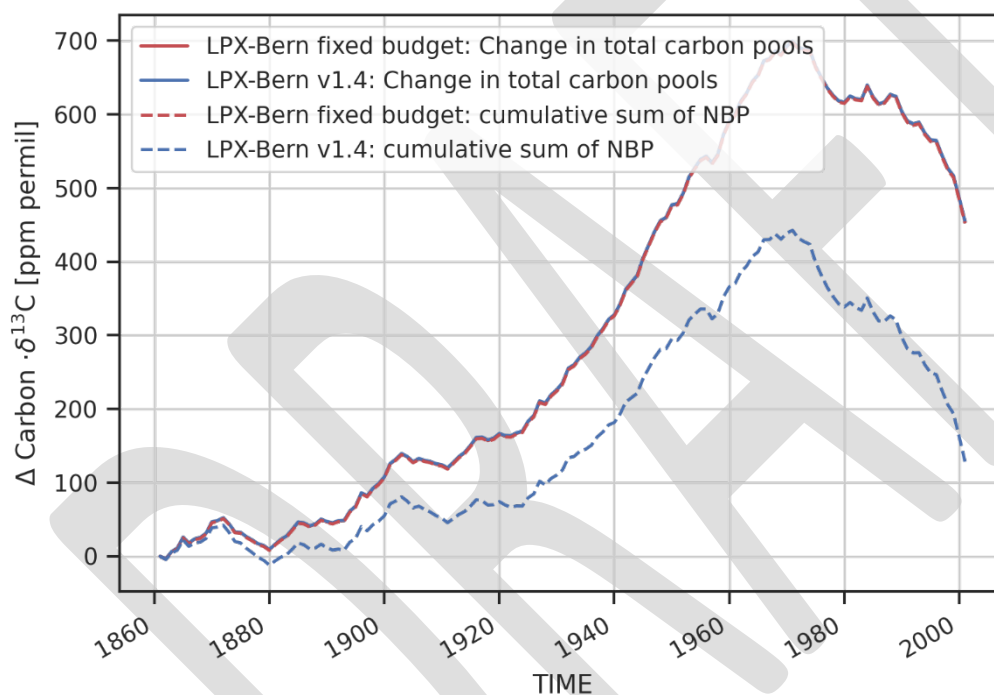
Figure 2: The global change in δ¹³C(CO₂) signature weighted total carbon as simulated by LPX-Bern over the historical period. Dashed lines correspond to the cumulative sum of net biome production (NBP), whereas solid lines show the change implied by the total carbon inventory. In blue the result of a simulation with the default model version is shown. The simulation with various fixes pertaining to the ¹³C budget (red), produces coinciding cumulative net biome production and total carbon inventory change.

In Figure 2 the globally integrated product of the change in total land carbon with its signature (ΔCarbon $\delta^{13}C$) is displayed, obtained by considering the change in the carbon reservoirs and integrating the net biome productivity (NBP). These two ways of computation should yield the same result; however, it is evident that

there is a large discrepancy between the two. Through step by step evaluation of the model code, multiple errors in the code were identified and fixed. For brevity's sake, we forgo detailing all the necessary code changes and instead provide one example: Daily net primary production (NPP) is reduced by the allocation of carbon to exudates, if and only if NPP is positive. An exudate pool accumulates carbon during the year and the signature is updated only if NPP is larger than 0. At the end of the year, the reduced NPP is allocated to biomass. However, the signature of the allocated biomass used the unreduced NPP, not considering that the allocation to exudates only if NPP is positive implied a signature change for the reduced NPP. The rectifying of this and other errors in the code solved the diverging $\Delta \mathrm{Carbon}\ \delta^{13}\mathrm{C}$, as is visible in Figure 2.

Similar to the discrepancy in $\Delta \mathrm{Carbon}\ \delta^{13}\mathrm{C}$, the signature of monthly NBP was not consistent with the signature of annual NBP. This problem was solved by correctly accounting for the signature of harvested carbon in heterotrophic respiration.

1.3 Distributing Litterfall

In LPX-Bern certain processes, such as the allocation of carbon from photosynthesis to biomass, mortality of plants, or litterfall, only take place at the end of the model year. In the current model version, the carbon reallocated by these processes is added immediately (in the first time step of the next model year) to the appropriate carbon pools. In the case of carbon added to litter pools, this is problematic when considering the seasonal cycle of CO_2 or $^{13}CO_2$. The sudden addition of large amounts of carbon to the litter pool at the end of the model year leads to increased heterotrophic respiration in the following months, most notably in January. This manifests as jumps from December to January when comparing the seasonal cycle of CO_2 and $\delta^{13}\mathrm{C}(CO_2)$ to observations.

We were able to mitigate this problem by distributing the end of year additions over the course of the year. The signature and amount of carbon in the litter pools is saved before the execution of the end of year processes. At the beginning of the next model year, the implied change in litter carbon signature and pools is calculated and then reverted. A fraction of the carbon is then added back each month, according to its length. This procedure has eliminated the observed discontinuity in NBP between December and January.

2 Simulation of the seasonal cycle of δ¹³C

The seasonal cycle of $\delta^{13}C(CO_2)$ is an important aspect of atmospheric in-situ measurements of $\delta^{13}C(CO_2)$, and a prime candidate for a novel observational constraint. Via the use of a model of atmospheric transport, simulated surface-to-atmosphere net carbon fluxes can be translated into local anomalies. Here we employ the TM3 atmospheric transport model (Heimann and Körner, 2003) to translate fluxes simulated by LPX-Bern and Bern3D, as well as estimated fluxes from fossil fuel emissions (Andres, Boden and Marland, 2017; Friedlingstein *et al.*, 2019) into local anomalies at 17 measurements station across the globe. The TM3 model code was modified to account for the difference in molar mass of ^{13}C compared to ^{12}C. Various modes of transport were tested (e.g. transporting the signature $\delta^{13}C(CO_2)$ and $^{12}CO_2$, or transporting $^{13}CO_2$ and $^{12}CO_2$) to achieve a numerically stable scheme.
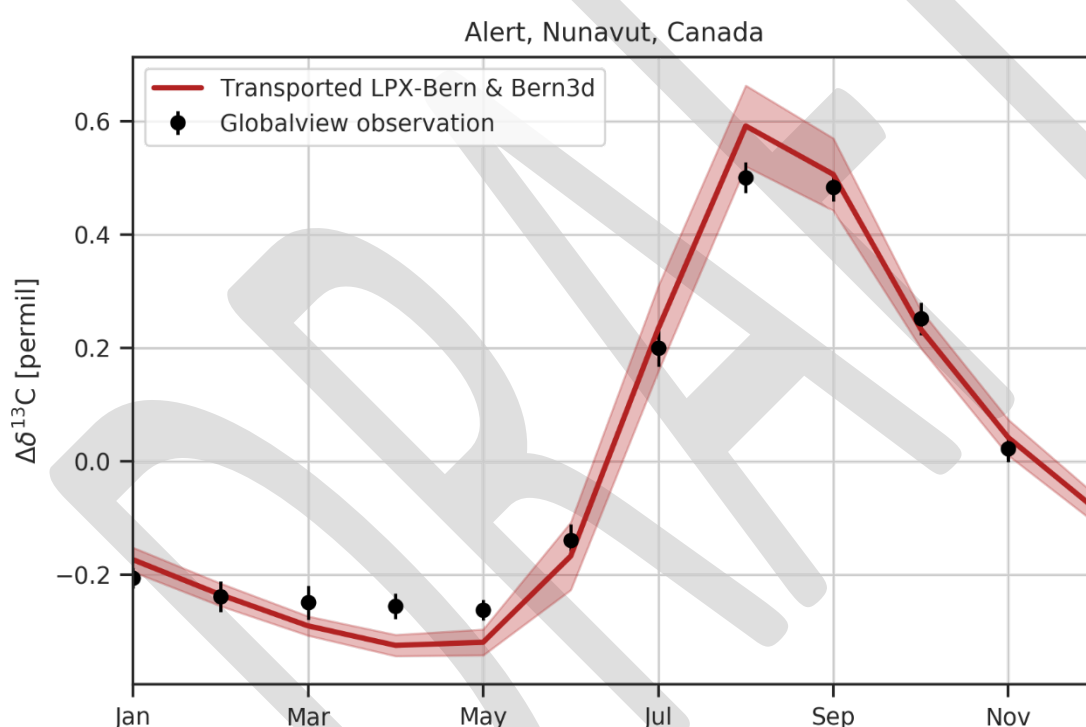
Figure 3: The seasonal cycle of δ¹³C(CO₂) at a measurement station located in Alert, Canada, between 1982 and 2013. In red the fluxes simulations by LPX-Bern and Bern3D including estimated fossil fuel fluxes, transported by the atmospheric transport model TM3, with standard deviation shaded in light red. Black dots with bars show in-situ measurements with their uncertainty indicated by black bars.

In Figure 3 the result of a Bern3D and LPX-Bern simulation transported with the TM3 model compared to an in-situ observation from Alert (GLOBALVIEW-CO2C13, 2009) is shown. Overall, there is a reasonable agreement between measurement and observation, giving a first indication of the potential of this technique. The sensitivity

of the seasonal changes to the model changes proposed in section 1 is currently being investigated by performing additional simulations. Furthermore, the sensitivity of the seasonal amplitude to changes in parametrization will be explored using factorial simulations.

3 Simulated atmospheric ^{13}C Budget

In addition to the seasonal cycle discussed in section 2, the overall atmospheric $^{13}CO_2$ budget is an important tool to evaluate model performance. The cumulative and globally integrated fluxes from land and ocean to atmosphere combined with the emissions from the burning of fossil fuels should equal the observed atmospheric growth in $^{13}CO_2$.

In Figure 4, this comparison is displayed using land-to-atmosphere fluxes from LPX-Bern, ocean-to-atmosphere fluxes from Bern3D and fossil fuel emissions as provided by CDIAC (Andres, Boden and Marland, 2017). Overall, there is a reasonable agreement between observation and simulation. In the considered period, the emissions from the burning of fossil fuels are opposed by an uptake of $^{13}CO_2$ by the ocean and a smaller uptake by the land.

While this broad agreement is encouraging, the next step will be to check that observed atmospheric $\delta^{13}C(CO_2)$ is compatible with the $\delta^{13}C(CO_2)$ implied by the model simulations. This measure is considerably more challenging to represent than the evolution of $^{13}CO_2$, which behaves similar as CO_2.

4 Outlook

UBern is on track to complete the tasks outlined in T1.1.3. One of the next milestones will be writing a paper, focusing on the merits of seasonal atmospheric $\delta^{13}C(CO_2)$ as an observational constraints for carbon cycle models. This study will also incorporate the results of factorial simulations, which will be performed and analysed in the near future. The factorial simulations will be used to explore the parameter and process dependence of the seasonal cycle of atmospheric $\delta^{13}C(CO_2)$. We have also taken first steps to extend the scope of the analysis from the EMIC Bern3D-LPX to the Community Earth System Model version 2 (CESM2). The results of an isotope enabled simulation using CESM may be incorporated in the study.

The industrial period change in atmospheric $\delta^{13}C(CO_2)$, will be considered as an additional observational constraint further down the line. We will also perform large model ensemble runs to further explore the parameter dependency of modelled $\delta^{13}C$, using a Bayesian approach.
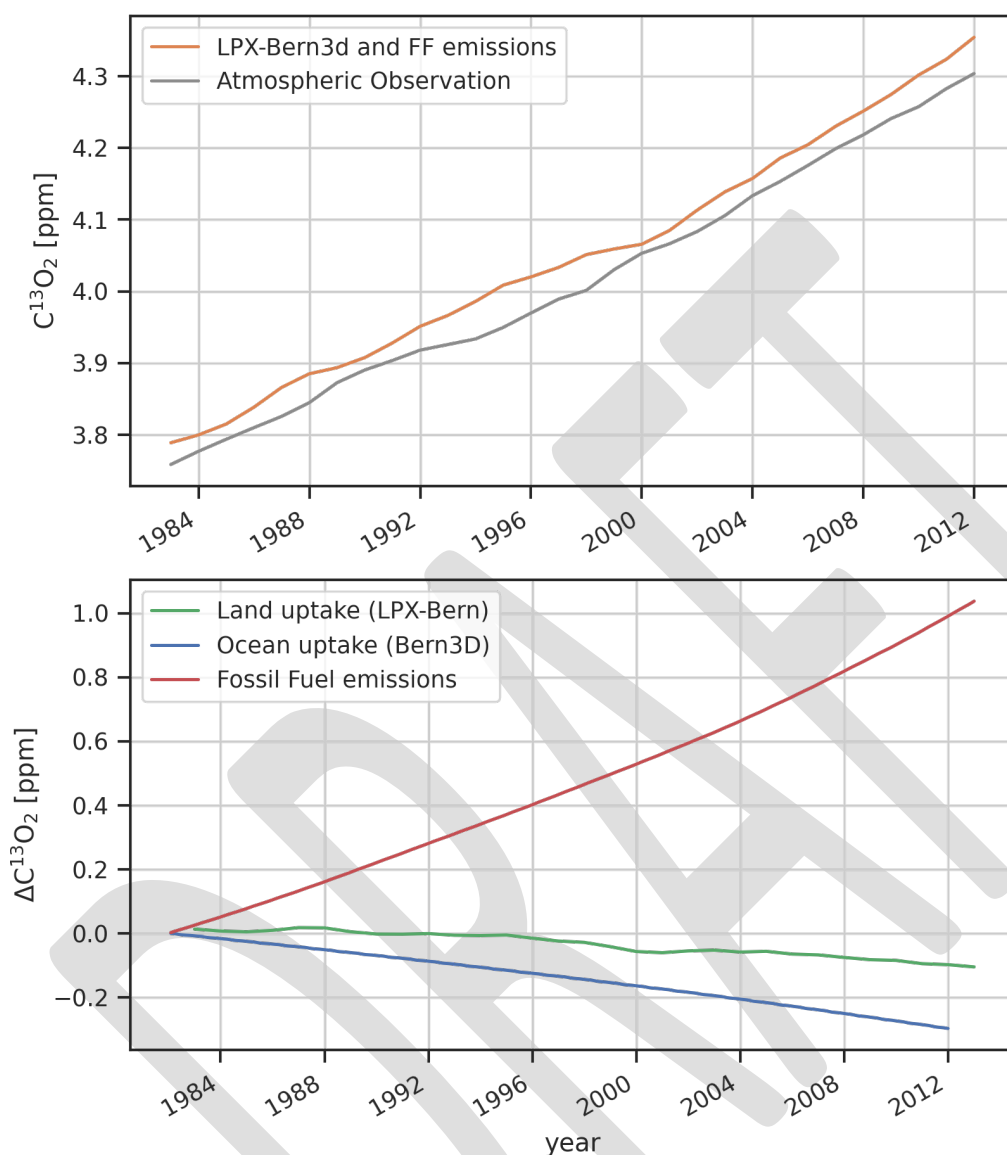
Figure 4: In the top, the change in atmospheric $^{13}CO_2$ (grey) is compared to the change implied by the spatially integrated fluxes (orange) from the land (LPX-Bern), ocean (Bern3D), and fossil fuel emissions (CDIAC). In the lower panel, the components of the implied atmospheric growth are displayed. In blue the ocean sink as simulated by Bern3D, in green the land sink as simulated by LPX-Bern, and in red the atmospheric growth due to fossil fuel emissions.

References

Andres, R., Boden, T. and Marland, G. (2017) 'Annual Fossil-Fuel CO2 Emissions: Global Stable Carbon Isotopic Signature'. CDIAC. doi: 10.3334/CDIAC/FFE.DB1013.2017.

Friedlingstein, P. *et al.* (2019) 'Global carbon budget 2019', *Earth System Science Data*, 11(4), pp. 1783–1838. doi: 10.5194/essd-11-1783-2019.

GLOBALVIEW-CO2C13 (2009) 'Cooperative Atmospheric Data Integration Project - δ13C of Carbon Dioxide.' NOAA ESRL, Boulder, Colorado.

Heimann, M. and Körner, S. (2003) *The Global Atmospheric Tracer Model TM3*. Max-Planck-Institut für Biogeochemie, Jena (Germany).

Hurtt, G. C. *et al.* (2020) 'Harmonization of global land use change and management for the period 850–2100 (LUH2) for CMIP6', *Geoscientific Model Development*, 13(11), pp. 5425–5464. doi: 10.5194/gmd-13-5425-2020.

Keller, K. M. *et al.* (2017) '20th century changes in carbon isotopes and water-use efficiency: tree-ring-based evaluation of the CLM4.5 and LPX-Bern models', *Biogeosciences*, 14(10), pp. 2641–2673. doi: 10.5194/bg-14-2641-2017.

Lienert, S. and Joos, F. (2018) 'A Bayesian ensemble data assimilation to constrain model parameters and land-use carbon emissions', *Biogeosciences*, 15(9), pp. 2909–2930. doi: 10.5194/bg-15-2909-2018.

Menviel, L., Joos, F. and Ritz, S. P. (2012) 'Simulating atmospheric CO2,13C and the marine carbon cycle during the Last Glacial-Interglacial cycle: Possible role for a deepening of the mean remineralization depth and an increase in the oceanic nutrient inventory', *Quaternary Science Reviews*. Elsevier Ltd, 56, pp. 46–68. doi: 10.1016/j.quascirev.2012.09.012.

Ritz, S. P. *et al.* (2011) 'A Coupled Dynamical Ocean–Energy Balance Atmosphere Model for Paleoclimate Studies', *Journal of Climate*, 24(2), pp. 349–375. doi: 10.1175/2010JCLI3351.1.

Scholze, M. *et al.* (2003) 'Climate and interannual variability of the atmosphere-biosphere 13 CO 2 flux', *Geophysical Research Letters*. 2000 FLORIDA AVE NW, WASHINGTON, DC 20009 USA: AMER GEOPHYSICAL UNION, 30(2). doi: 10.1029/2002GL015631.

Scholze, M., Ciais, P. and Heimann, M. (2008) 'Modeling terrestrial13C cycling: Climate, land use and fire', *Global Biogeochemical Cycles*, 22(1), pp. 1–13. doi: 10.1029/2006GB002899.

Sitch, S. *et al.* (2003) 'Evaluation of ecosystem dynamics, plant geography and terrestrial carbon cycling in the LPJ dynamic global vegetation model', *Global Change Biology*, 9(2), pp. 161–185. doi: 10.1046/j.1365-

2486.2003.00569.x.

Suits, N. S. *et al.* (2005) 'Simulation of carbon isotope discrimination of the terrestrial biosphere', *Global Biogeochemical Cycles*, 19(1), pp. 1–15. doi: 10.1029/2003GB002141.